

## THE CRYSTAL CHEMISTRY OF THE GRAFTONITE-BEUSITE MINERALS

KIMBERLY T. TAIT\* AND FRANK C. HAWTHORNE§

*Department of Geological Sciences, University of Manitoba, Winnipeg, Manitoba, Canada R3T 2N2*

MICHAEL A. WISE

*Department of Mineral Sciences, Smithsonian Institution, Washington, D.C. 20560, U.S.A.*

### ABSTRACT

The crystal structures of seven members of the graftonite-beusite series, ideally  $(\text{Fe}^{2+}, \text{Mn}^{2+}, \text{Ca})_3(\text{PO}_4)_2$ , monoclinic  $P2_1/c$ ,  $a$  8.77–8.81,  $b$  11.43–11.58,  $c$  6.13–6.17 Å,  $\beta$  99.19–99.32°,  $V$  607.5–617.7 Å<sup>3</sup>, have been refined to  $R_1$  indices of 2.1–3.7% using ~1300–1600 unique observed reflections ( $|F_o| > 5\sigma F$ ) collected using a single-crystal diffractometer equipped with MoK $\alpha$  X-radiation. The crystals used in the collection of the X-ray data were subsequently analyzed with an electron microprobe and the structural and microprobe results were used to assign site populations. The refined site-scattering values and linear variation in mean bond-length as a function of aggregate-cation radius indicate that Ca is completely ordered at the  $M(1)$  site. Similarly, Mn is ordered at the  $M(1)$  and  $M(3)$  sites, with any excess Mn occurring at  $M(2)$ , and Mg is completely ordered at  $M(2)$ . Detailed consideration of incident bond-valence sums at the three  $M$  sites indicates that the coordination numbers of the  $M(1)$ ,  $M(2)$ , and  $M(3)$  sites are [8], [5], and [6], respectively, although the differences between these and [7], [5], and [5] are very small. Ca is dominant at the  $M(1)$  site in a previously refined beusite structure, and there are compositions reported here and elsewhere in which Ca is dominant at  $M(1)$  in graftonite-like compositions, indicating the potential for new mineral species in this group.

*Keywords:* Graftonite, beusite, crystal-structure refinement, electron-microprobe data.

### INTRODUCTION

Graftonite, ideally  $[\text{Fe}^{2+}_3(\text{PO}_4)_2]$ , was described by Penfield (1900) from a granitic pegmatite in New Hampshire. Beusite, ideally  $[\text{Mn}^{2+}_3(\text{PO}_4)_2]$ , was first noted by Beus (1950) and Brooks & Shipway (1960) as a graftonite-like mineral with  $\text{Mn}^{2+}$  dominant over  $\text{Fe}^{2+}$ , and was formally described as a distinct species from the pegmatites of the San Luis area, Argentina, by Hurlbut & Aristarain (1968). Both minerals form a solid-solution series and occur commonly as late-stage accessory minerals in complex granitic pegmatites (*e.g.*, Franolet 1977, Franolet *et al.* 1986, Lahti 1981, Wise & Černý 1990, Wise *et al.* 1990, Černý *et al.* 1998, Smeds *et al.* 1998, Pieczka 2007, Guastoni *et al.* 2007, Vignola *et al.* 2008, Galliski *et al.* 2009, Ericit *et al.* 2010). These minerals also occur as constituents of phosphate-oxide inclusions in IIIAB iron meteorites (Bild 1974, Olsen *et al.* 1999), and graftonite has been reported as a primary phase in a phosphorous-rich iron formation (Stalder & Rozendaal 2002).

The graftonite-beusite structure is a dense framework of polyhedra, with extensive edge- and corner-sharing (Hawthorne 1998, Huminicki & Hawthorne 2002) between phosphate tetrahedra and [5]- to [8]-coordinated divalent-metal-oxide polyhedra. The crystal structure of graftonite was solved by Calvo (1968) and beusite by Hurlbut & Aristarain (1968). The chemical composition of this series may be written as  $(\text{Fe}^{2+}, \text{Mn}^{2+}, \text{Ca})_3(\text{PO}_4)_2$ , and Ca plays an important role in the structure of these minerals. In this structure, there are three distinct divalent-metal sites:  $M(1)$ ,  $M(2)$ , and  $M(3)$ . Calvo (1968) described the coordination of these sites as [7], [5], and [5], respectively, with Ca preferentially occupying the  $M(1)$  site. With decreasing Ca content, it has been suggested that the coordination of the  $M(1)$  site tends to decrease from [7] to [6] to [5] (Calvo 1968, Wise *et al.* 1990, Steele *et al.* 1991). The  $M(2)$  site has been reported as [5]-coordinated and tends to be  $\text{Fe}^{2+}$ -dominant (Nord & Ericsson 1982);  $M(3)$  has been described as both [5]- and [6]-coordinated, and tends to be  $\text{Mn}^{2+}$ -dominant. Wise *et al.* (1990) reported

\* Current address: Department of Natural History, Mineralogy, Royal Ontario Museum, 100 Queen's Park, Toronto, Ontario M5S 2C6, Canada

§ Corresponding author: frank\_hawthorne@umanitoba.ca

a Ca-rich beusite where Ca dominates the  $M(1)$  site. The coordinations of the divalent cations in the graffonite-beusite minerals are unusual in that they show a wide range of M–O bond-lengths that make the actual coordination numbers difficult to determine uniquely. Here, we report detailed crystallographic results for seven samples with varying chemical composition to study the cation order and variation of the coordination at each of the  $M(1)$ ,  $M(2)$ , and  $M(3)$  sites.

### EXPERIMENTAL

The provenance of all samples used in the present work is given in Table 1. Fragments from all seven samples were rounded with an air-driven crystal grinder, attached to glass fibers, and mounted on a Bruker  $P4$  automated four-circle diffractometer equipped with  $\text{MoK}\alpha$  X-radiation. Fifty reflections over the range  $15 \leq 2\theta \leq 40^\circ$  were centered, and the unit-cell parameters (Table 2) were refined by least squares from the resultant setting angles. Intensities were measured from 4 to  $60^\circ 2\theta$  ( $13 \leq h \leq 13, 0 \leq k \leq 13, 0 \leq l \leq 13$ ) with scan

speeds varying between 2.0 and  $29.3^\circ 2\theta/\text{min}$ . Intensities were corrected for Lorentz, polarization and background effects, and reduced to structure factors; the numbers of observed reflections ( $|F_o| \geq 5\sigma F$ ) are reported in Table 2. Subsequent to the diffraction experiment, the crystals used for collection of the X-ray intensity data were analyzed with a Cameca SX-50 electron microprobe according to the procedure of Hawthorne *et al.* (1993). Eight to ten points (depending on crystal size) were acquired ( $20 \mu\text{m}$  beam-size) uniformly across each sample; the results are reported in Table 3, together with the unit formulae calculated on the basis of 8 O *apfu* (atoms per formula unit).

### STRUCTURE REFINEMENT

All calculations were done with the SHELXTL PC (Plus) system of programs;  $R$  indices are expressed as percentages. In the refinement of the site-scattering values, Ca and Mn were assigned to the  $M(1)$  site, Fe was assigned to the  $M(2)$  site, and Mn was assigned to the  $M(3)$  site. The relative occupancies of Ca and

TABLE 1. DETAILS OF SAMPLE NUMBER AND PROVENANCE FOR GRAFTONITE-BEUSITE SAMPLES

Crystal no.	Smithsonian catalog no.	IMA name	Pegmatite Provenance
B1	NMNH 107378	graffonite	Lollington beryl mine, Karoi, Hurungwe, Zimbabwe
B2	NMNH 157355	beusite	Rice mine, North Groton, Grafton Co., New Hampshire, U.S.A.
B3	NMNH R19015	beusite	Los Aleros, San Luis, Argentina
B4	NMNH 112665	beusite	Turkestan Range, Kyrgyzstan
B5	NMNH 161645	graffonite	Palermo mine, North Groton, Grafton Co., New Hampshire, U.S.A.
B6	NMNH 144089	graffonite	Mwami district, Hurungwe, Zimbabwe
B7	NMNH 143142	graffonite	East Alstead, New Hampshire, U.S.A.

TABLE 2. MISCELLANEOUS DATA-COLLECTION AND STRUCTURE-REFINEMENT INFORMATION FOR BEUSITE AND GRAFTONITE

	B1	B2	B3	B4	B5	B6	B7
$a$ (Å)	8.8052(5)	8.7900(5)	8.7919(4)	8.775(1)	8.7994(4)	8.788(2)	8.8072(6)
$b$	11.4793(4)	11.5382(6)	11.5414(5)	11.437(2)	11.5702(5)	11.583(2)	11.5131(7)
$c$	6.1388(5)	6.1654(5)	6.1669(4)	6.133(1)	6.1365(4)	6.141(2)	6.1372(6)
$\beta$ (°)	99.192(6)	99.199(5)	99.188(5)	99.192(4)	99.320(4)	99.30(2)	99.243(6)
$V$ (Å <sup>3</sup> )	612.53(7)	617.26(7)	617.73(6)	607.54(6)	616.52(6)	616.9(2)	614.23(8)
Space group	$P2_1/c$	$P2_1/c$	$P2_1/c$	$P2_1/c$	$P2_1/c$	$P2_1/c$	$P2_1/c$
Crystal size ( $\mu\text{m}$ )	$80 \times 120 \times 80$	$120 \times 140 \times 160$	$80 \times 120 \times 80$	$40 \times 80 \times 40$	$80 \times 120 \times 100$	$60 \times 80 \times 60$	$40 \times 40 \times 40$
$\mu\text{m}$ ( $\text{mm}^{-1}$ )	6.6	5.7	5.8	6.5	6.1	6.3	6.4
No. of $ F $	1802	1818	1819	1792	1813	1817	1809
No. of $ F_o  > 5\sigma F$	1489	1598	1466	1592	1573	1336	1298
$R(\text{merge})$ %	2.4	1.0	2.0	1.6	0.9	3.7	1.5
$R(\text{obs})$ %	2.2	2.1	2.8	2.6	2.6	3.7	3.4
$wR(\text{obs})$ %	2.3	2.2	3.0	2.8	2.6	3.9	3.6

TABLE 3. CHEMICAL COMPOSITIONS (WT.%) AND FORMULAE (*apfu*) OF BEUSITE AND GRAFTONITE CRYSTALS

	B1	B2	B3	B4	B5	B6	B7
P <sub>2</sub> O <sub>5</sub>	40.39	41.25	40.92	41.09	41.00	40.57	40.46
MnO	26.09	35.77	34.71	26.86	12.49	16.30	20.25
FeO	28.34	13.45	13.42	25.09	34.26	32.27	30.32
CaO	4.12	5.68	5.64	3.14	9.35	9.04	5.84
MgO	0.25	2.38	2.33	2.79	1.72	0.30	1.24
ZnO	0.28	0.36	0.33	0.14	0.21	0.13	0.09
Σ	99.48	98.89	97.35	99.11	99.04	98.63	98.22
Chemical formulae							
Mn <sup>2+</sup>	1.297	1.747	1.717	1.316	0.610	0.807	1.006
Fe <sup>2+</sup>	1.391	0.648	0.655	1.213	1.652	1.577	1.488
Ca	0.259	0.351	0.353	0.195	0.578	0.566	0.367
Mg	0.022	0.205	0.203	0.241	0.148	0.026	0.108
Zn	0.012	0.015	0.014	0.006	0.009	0.006	0.004
Σ	2.980	2.965	2.941	2.970	2.997	2.981	2.972
P	2.007	2.013	2.023	2.012	2.001	2.007	2.010
O	8	8	8	8	8	8	8

Mn were refined at *M*(1) and the occupancies of Fe and Mn were refined at *M*(2) and *M*(3), respectively. Refinement converged to *R* indices of 2.1–3.7% for a model with anisotropic-displacement parameters for all atoms and using ionic scattering factors for all atoms except P. Final atom positions and displacement parameters are given in Table 4, selected interatomic distances are listed in Table 5, and refined site-scattering values (Hawthorne *et al.* 1995) are given in Table 6. A bond-valence table for crystal B1 is given in Table 7, calculated with the parameters of Brown & Altermatt (1985). Observed and calculated structure-factors are available from the Depository of Unpublished Data, on the MAC website [document CM\_653].

#### SITE POPULATIONS

There are four scattering species, Mg, Ca, Mn, and Fe, to be distributed over three *M*-sites. This cannot be done unambiguously from the refined site-scattering values (Hawthorne 1983) and we must also appeal to criteria involving mean bond-lengths and constituent cation radii, which in turn are a function of cation coordination number. However, for the graftonite-beusite minerals, the coordination numbers of the *M* sites are somewhat uncertain (Calvo 1968, Steele *et al.* 1991, Wise *et al.* 1990), and using the valence-sum rule (Brown 2002, Hawthorne & Schindler 2008) requires knowledge of the site populations. Therefore deciding on coordination numbers and deriving site populations need to be interactive processes.

#### Initial assignment of site populations

We will begin this process with the coordination numbers [8], [5], and [6] for the *M*(1), *M*(2), and *M*(3) sites, respectively. The  $\langle M(1)-O \rangle$  distances are much larger than the other  $\langle M-O \rangle$  distances (Table 5), indicating that Ca occupies the *M*(1) site, and previous work (Wise *et al.* 1990) has assigned Ca to *M*(1). The refinement of several graftonite-beusite structures of different Ca content (Table 3) allows us to test this assignment in a more quantitative manner. Calcium is much larger than Mn<sup>2+</sup>, Fe<sup>2+</sup>, and Mg for all coordination numbers [e.g., for [8]-coordination, Ca = 1.12, Mn<sup>2+</sup> = 0.96, Fe<sup>2+</sup> = 0.92, and Mg = 0.89 Å (Shannon 1976)], and if Ca is ordered at *M*(1), there should be a positive correlation between the Ca content of the structure and the  $\langle M(1)-O \rangle$  distance. As shown in Figure 1, this is the case: the data of the present work lie on a straight line between the data of Steele *et al.* (1991) with Ca = 0.00 *apfu*, and that of Wise *et al.* (1990) with Ca = 0.98 *apfu*. Thus all Ca was assigned to *M*(1).

The site-scattering values at the *M*(3) site are ~25 *epfu* (Table 6), indicating occupancy of *M*(3) by Mn and Fe only, whereas the site-scattering values at the *M*(2) site range from 23.4 to 25.8 *epfu*; as Mg is the only remaining scattering species with a scattering factor < 25 e, Mg must occur at the *M*(2) site. Accordingly, the refined site-scattering at the *M*(2) site decreases with increasing Mg content in the crystal (Fig. 2). There is considerable scatter in this plot, but this presumably arises from variations in Mn *versus* Fe content as the

TABLE 4. ATOM POSITIONS AND EQUIVALENT ISOTROPIC-DISPLACEMENT PARAMETERS ( $\times 10^4$ ) FOR BEUSITE AND GRAFTONITE

Site		B1	B2	B3	B4	B5	B6	B7
M(1)	x	0.94535(6)	0.94364(5)	0.94370(7)	0.94419(6)	0.94689(7)	0.9476(1)	0.9455(1)
	y	0.11865(4)	0.11988(4)	0.11994(5)	0.11872(5)	0.12106(5)	0.12126(8)	0.11950(8)
	z	0.84046(8)	0.83899(7)	0.8390(1)	0.84167(9)	0.8353(1)	0.8341(2)	0.8386(2)
	$U_{\text{eq}}$	160(1)	162(1)	159(2)	173(2)	183(2)	166(3)	172(3)
M(2)	x	0.71810(5)	0.71692(5)	0.71679(7)	0.71860(7)	0.71459(6)	0.7144(1)	0.7168(1)
	y	0.07925(5)	0.0766(4)	0.07653(6)	0.07877(5)	0.07890(5)	0.07933(8)	0.07885(8)
	z	0.32868(7)	0.32915(7)	0.32916(9)	0.32887(8)	0.32693(7)	0.3270(1)	0.3281(1)
	$U_{\text{eq}}$	183(1)	179(1)	174(2)	193(2)	200(2)	180(3)	199(3)
M(3)	x	0.36257(5)	0.36044(4)	0.36041(6)	0.36230(6)	0.36254(5)	0.36189(9)	0.36221(9)
	y	0.19136(4)	0.19111(3)	0.19110(5)	0.19145(4)	0.19167(4)	0.19124(7)	0.19137(7)
	z	0.12774(7)	0.12860(6)	0.12858(8)	0.12731(7)	0.12930(7)	0.1300(1)	0.1284(1)
	$U_{\text{eq}}$	107(1)	120(1)	118(2)	124(1)	120(1)	116(2)	116(2)
P(1)	x	0.09257(8)	0.09038(7)	0.0902(1)	0.09188(9)	0.09484(8)	0.0943(2)	0.0932(1)
	y	0.13584(6)	0.13580(5)	0.13591(7)	0.13604(7)	0.13441(6)	0.1343(1)	0.1351(1)
	z	0.3951(1)	0.39342(9)	0.3934(1)	0.3941(1)	0.3964(1)	0.3968(2)	0.3955(2)
	$U_{\text{eq}}$	85(2)	93(2)	90(2)	102(2)	103(2)	105(3)	98(3)
P(2)	x	0.60412(8)	0.60285(7)	0.6028(2)	0.60403(9)	0.60217(8)	0.6020(1)	0.6031(1)
	y	0.08855(6)	0.08864(5)	0.08865(7)	0.08825(7)	0.08854(6)	0.0890(1)	0.0886(1)
	z	0.8070(1)	0.80689(9)	0.8070(1)	0.8069(1)	0.8065(1)	0.8070(2)	0.8066(2)
	$U_{\text{eq}}$	81(2)	91(2)	86(2)	98(2)	92(2)	94(3)	91(3)
O(1)	x	0.0769(2)	0.07704(2)	0.0771(3)	0.0768(3)	0.0800(3)	0.0795(5)	0.0784(4)
	y	0.0680(2)	0.0688(2)	0.0687(2)	0.06789(2)	0.0691(2)	0.0698(3)	0.0681(3)
	z	0.1770(3)	0.1769(3)	0.1764(4)	0.1764(4)	0.1775(3)	0.1771(6)	0.1769(5)
	$U_{\text{eq}}$	134(5)	151(5)	139(7)	154(6)	157(6)	167(10)	156(10)
O(2)	x	0.4777(2)	0.4756(2)	0.4757(3)	0.4777(3)	0.4731(2)	0.4737(4)	0.4762(4)
	y	0.1770(2)	0.1768(2)	0.1770(2)	0.1773(2)	0.1751(2)	0.1749(3)	0.1765(3)
	z	0.8301(3)	0.8307(3)	0.8311(4)	0.8292(4)	0.8293(3)	0.8296(6)	0.8294(5)
	$U_{\text{eq}}$	130(5)	138(5)	141(7)	139(6)	133(6)	140(10)	134(9)
O(3)	x	0.9414(2)	0.9372(2)	0.9368(3)	0.9402(3)	0.9419(3)	0.9415(5)	0.9415(4)
	y	0.1988(2)	0.1954(2)	0.1957(3)	0.1990(2)	0.1926(2)	0.1922(4)	0.1965(4)
	z	0.4158(4)	0.4158(3)	0.4154(5)	0.4131(4)	0.4233(4)	0.4245(7)	0.4185(6)
	$U_{\text{eq}}$	196(6)	210(6)	201(8)	205(7)	229(7)	215(12)	224(12)
O(4)	X	0.6951(2)	0.6927(2)	0.6930(3)	0.6954(3)	0.6898(2)	0.6894(4)	0.6927(4)
	Y	0.1267(2)	0.1275(2)	0.1276(2)	0.1260(2)	0.1267(2)	0.1274(3)	0.1271(3)
	Z	0.6257(3)	0.6257(3)	0.6257(4)	0.6258(4)	0.6226(3)	0.6223(6)	0.6237(5)
	$U_{\text{eq}}$	123(5)	137(5)	144(7)	142(6)	138(6)	134(10)	138(10)
O(5)	X	0.2185(3)	0.2124(2)	0.2126(3)	0.2184(3)	0.2169(3)	0.2159(5)	0.2172(5)
	Y	0.2276(2)	0.2302(2)	0.2300(3)	0.2280(2)	0.2288(2)	0.2300(4)	0.2281(3)
	Z	0.3807(3)	0.3789(3)	0.3790(4)	0.3797(4)	0.3832(4)	0.3832(6)	0.3816(6)
	$U_{\text{eq}}$	172(6)	179(5)	183(8)	193(7)	195(6)	186(11)	184(11)
O(6)	X	0.7268(2)	0.7256(2)	0.7260(3)	0.7267(3)	0.7256(2)	0.7258(4)	0.7265(4)
	Y	0.0878(2)	0.0873(2)	0.2300(3)	0.0868(2)	0.0901(2)	0.0901(3)	0.0887(3)
	Z	0.0156(3)	0.0147(3)	0.0145(4)	0.0159(4)	0.0149(3)	0.0149(6)	0.0153(5)
	$U_{\text{eq}}$	124(5)	131(5)	128(7)	146(6)	130(5)	136(10)	127(9)
O(7)	X	0.1354(3)	0.1369(2)	0.1367(3)	0.1345(3)	0.1417(3)	0.1412(5)	0.1383(5)
	Y	0.0612(2)	0.0615(2)	0.0609(2)	0.0612(2)	0.0591(2)	0.0595(3)	0.1383(5)
	Z	0.6002(4)	0.5967(3)	0.5970(4)	0.5998(4)	0.5994(4)	0.5988(7)	0.6003(6)
	$U_{\text{eq}}$	183(6)	199(5)	187(8)	189(7)	181(6)	189(11)	202(11)
O(8)	X	0.5338(2)	0.5328(2)	0.5326(3)	0.5332(3)	0.5351(2)	0.5349(4)	0.5338(4)
	Y	-0.0344(2)	-0.0335(2)	-0.0334(2)	-0.0349(2)	-0.0350(2)	-0.0344(3)	-0.0344(3)
	Z	0.7612(3)	0.7602(3)	0.7596(4)	0.7606(4)	0.7644(3)	0.7629(6)	0.7625(5)
	$U_{\text{eq}}$	116(5)	125(5)	121(7)	139(6)	125(5)	122(10)	112(9)

TABLE 5. SELECTED INTERATOMIC DISTANCES (Å) FOR BEUSITE AND GRAFTONITE

	B1	B2	B3	B4	B5	B6	B7
<i>M</i> (1)–O(1)a	2.276(2)	2.298(2)	2.297(2)	2.267(2)	2.313(2)	2.312(4)	2.291(4)
<i>M</i> (1)–O(1)b	2.152(2)	2.186(2)	2.186(3)	2.143(2)	2.213(2)	2.227(4)	2.170(4)
<i>M</i> (1)–O(3)	2.759(2)	2.743(2)	2.746(3)	2.780(3)	2.654(3)	2.638(4)	2.721(5)
<i>M</i> (1)–O(3)c	2.148(2)	2.186(2)	2.183(3)	2.131(3)	2.226(3)	2.235(5)	2.176(5)
<i>M</i> (1)–O(4)	2.382(2)	2.382(2)	2.382(3)	2.365(2)	2.432(2)	2.428(4)	2.400(3)
<i>M</i> (1)–O(5)d	2.961(2)	2.907(2)	2.909(3)	2.958(3)	2.920(3)	2.897(4)	2.945(4)
<i>M</i> (1)–O(6)e	2.376(2)	2.377(2)	2.375(3)	2.361(2)	2.415(2)	2.422(4)	2.386(4)
<i>M</i> (1)–O(7)f	2.490(3)	2.526(2)	2.526(3)	2.495(3)	2.520(3)	2.507(5)	2.508(4)
< <i>M</i> (1)–O>	2.443(2)	2.451	2.451	2.438	2.462	2.458	2.450
<i>M</i> (2)–O(3)	2.387(2)	2.363(2)	2.363(3)	2.374(3)	2.386(2)	2.379(4)	2.389(4)
<i>M</i> (2)–O(4)	1.945(2)	1.964(2)	1.965(3)	1.940(2)	1.943(2)	1.943(4)	1.941(3)
<i>M</i> (2)–O(6)	1.938(2)	1.956(2)	1.959(3)	1.934(2)	1.938(2)	1.939(4)	1.939(3)
<i>M</i> (2)–O(7)b	2.067(2)	2.052(2)	2.048(3)	2.059(3)	2.042(2)	2.054(4)	2.047(4)
<i>M</i> (2)–O(8)b	2.258(2)	2.232(2)	2.230(3)	2.243(2)	2.236(2)	2.233(4)	2.247(3)
< <i>M</i> (2)–O>	2.119	2.113	2.113	2.110	2.109	2.110	2.113
<i>M</i> (3)–O(1)	2.944(2)	2.919(2)	2.920(3)	2.935(3)	2.919(2)	2.907(4)	2.931(4)
<i>M</i> (3)–O(2)g	2.233(2)	2.240(2)	2.239(3)	2.236(2)	2.225(2)	2.233(4)	2.235(4)
<i>M</i> (3)–O(2)h	2.110(2)	2.121(2)	2.122(3)	2.101(2)	2.108(2)	2.117(4)	2.108(3)
<i>M</i> (3)–O(5)	2.196(2)	2.218(2)	2.218(3)	2.185(3)	2.214(3)	2.216(4)	2.205(4)
<i>M</i> (3)–O(5)h	2.040(2)	2.061(2)	2.061(3)	2.033(2)	2.035(2)	2.037(4)	2.041(4)
<i>M</i> (3)–O(8)b	2.085(2)	2.110(2)	2.113(2)	2.079(2)	2.081(2)	2.089(4)	2.087(4)
< <i>M</i> (3)–O>	2.268	2.278	2.279	2.262	2.264	2.267	2.268
<i>P</i> (1)–O(1)	1.536(2)	1.531(2)	1.535(3)	1.533(2)	1.528(2)	1.529(4)	1.535(4)
<i>P</i> (1)–O(3)i	1.538(2)	1.538(2)	1.540(3)	1.534(3)	1.537(3)	1.535(4)	1.538(4)
<i>P</i> (1)–O(5)	1.542(2)	1.541(2)	1.541(3)	1.542(3)	1.543(3)	1.551(4)	1.541(4)
<i>P</i> (1)–O(7)	1.521(2)	1.520(2)	1.526(3)	1.520(2)	1.522(2)	1.514(4)	1.526(4)
< <i>P</i> (1)–O>	1.534	1.533	1.536	1.532	1.533	1.532	1.535
<i>P</i> (2)–O(2)	1.530(2)	1.536(2)	1.537(3)	1.528(2)	1.537(2)	1.528(4)	1.531(4)
<i>P</i> (2)–O(4)	1.535(2)	1.535(2)	1.537(3)	1.532(2)	1.531(2)	1.534(4)	1.538(4)
<i>P</i> (2)–O(6)e	1.538(2)	1.538(2)	1.539(3)	1.536(2)	1.538(2)	1.539(4)	1.541(3)
<i>P</i> (2)–O(8)	1.549(2)	1.546(2)	1.547(3)	1.548(2)	1.552(2)	1.552(4)	1.548(4)
< <i>P</i> (2)–O>	1.538	1.539	1.540	1.536	1.540	1.538	1.540

a:  $1+x, y, 1+z$ ; b:  $1-x, -y, 1-z$ ; c:  $x, \frac{1}{2}-y, \frac{1}{2}+z$ ; d:  $1+x, \frac{1}{2}-y, \frac{1}{2}+z$ ; e:  $x, y, 1+z$ ; f:  $1+x, y, z$ ; g:  $x, y, z-1$ ; h:  $x, \frac{1}{2}-y, z-\frac{1}{2}$ ; i:  $x-1, y, z$ .

total variation in *M*(2) site-scattering is only 2.4 e; the magnitude of this possible effect is shown by the shaded band in Figure 2. Thus all Mg was assigned to *M*(2).

This leaves Fe and Mn to be distributed over the *M*(2) and *M*(3) sites, which requires that the coordination numbers be known for *M*(2) and *M*(3). Examination of this issue (see below) shows that *M*(2) is [5]-coordinated and *M*(3) is [6]-coordinated. The appropriate <*M*(2)–O> and <*M*(3)–O> distances (Table 5) indicate that both Mn and Fe must be in the divalent state (in accord with the stoichiometry of the minerals). As Mn (*Z* = 25) and Fe (*Z* = 26) scatter X-rays in a very similar manner, we cannot use the refined site-scattering values to assign Mn<sup>2+</sup> and Fe<sup>2+</sup> site populations. However, Mn<sup>2+</sup> (*r* = 0.83 Å) is larger than Fe<sup>2+</sup> (*r* = 0.78 Å) (radii

from Shannon 1976), and the <*M*–O> bond-lengths will give an indication of their relative occupancies, particularly as the amount of Mg at the *M*(2) site is usually quite small. As a first step, all Mn<sup>2+</sup> was assigned to the *M*(3) site as the <*M*(3)–O> distances in all samples (~2.27 Å) are significantly longer than the <*M*(2)–O> distances (~2.11 Å). As shown in Figure 3, the resulting variation in mean bond-length as a function of constituent-cation radius is fairly linear for *M*(1) and *M*(3), except for sample B4 in the latter. The variation in <*M*(2)–O> is only ~0.01 Å, and as this is only 3–4 standard deviations of the <*M*(2)–O> distances, a well-developed linear trend is not expected here. The final assigned site populations are listed in Table 6.

TABLE 6. SITE-SCATTERING VALUES AND SITE POPULATIONS IN BEUSITE-GRAFTONITE

	Site	Site scattering (exp., <i>epfu</i> )	Site scattering (calc., <i>epfu</i> )	Site populations ( <i>apfu</i> )
B1	M(1)	23.8(3)	23.7	0.26 Ca + 0.74 Mn
	M(2)	25.6(1)	25.7	0.97 Fe + 0.02 Mg + 0.01 Zn
	M(3)	25.5(1)	25.4	0.43 Fe + 0.57 Mn
B2	M(1)	23.3(2)	23.2	0.36 Ca + 0.64 Mn
	M(2)	23.0(1)	23.0	0.67 Fe + 0.11 Mn + 0.21 Mg + 0.01 Zn
	M(3)	24.8(1)	25.0	1.00 Mn
B3	M(1)	23.3(3)	23.2	0.36 Ca + 0.64 Mn
	M(2)	23.2(2)	23.0	0.67 Fe + 0.11 Mn + 0.21 Mg + 0.01 Zn
	M(3)	25.0(1)	25.0	1.00 Mn
B4	M(1)	24.0(3)	24.0	0.20 Ca + 0.80 Mn
	M(2)	23.7(1)	22.6	0.75 Fe + 0.24 Mg + 0.01 Zn
	M(3)	24.5(1)	25.5	0.47 Fe + 0.53 Mn
B5	M(1)	22.1(3)	22.1	0.58 Ca + 0.42 Mn
	M(2)	24.5(1)	24.0	0.84 Fe + 0.15 Mg + 0.01 Zn
	M(3)	25.4(1)	25.8	0.81 Fe + 0.19 Mn
B6	M(1)	22.1(5)	22.2	0.57 Ca + 0.43 Mn
	M(2)	25.4(1)	25.7	0.97 Fe + 0.02 Mg + 0.01 Zn
	M(3)	25.4(1)	25.6	0.62 Fe + 0.38 Mn
B7	M(1)	23.1(5)	23.2	0.37 Ca + 0.63 Mn
	M(2)	24.9(1)	24.5	0.89 Fe + 0.11 Mg
	M(3)	25.3(1)	25.6	0.62 Fe + 0.38 Mn

TABLE 7. BOND-VALENCE (*vu*) TABLE FOR CRYSTAL B1

	M(1)	M(2)	M(3)	P(1)	P(2)	$\Sigma$
O(1)	0.294 0.473			1.280		2.047
O(2)			0.292 0.396		1.263	1.951
O(3)	0.387 0.111	0.197		1.256		1.951
O(4)	0.241	0.539			1.266	2.046
O(5)	0.081		0.308 0.466	1.245		2.100
O(6)	0.244	0.551			1.256	2.051
O(7)	0.175	0.426		1.320		1.921
O(8)		0.270	0.408		1.228	1.906
$\Sigma$	2.006	1.983	1.870	5.101	5.013	

*Cation-coordination numbers*

The coordination numbers for M(1) and M(3) are somewhat uncertain. With regard to the coordination number for M(2), the fifth-shortest M(2)–O distance

in these structures is  $\sim 2.38 \text{ \AA}$  ( $\sim 0.17 \text{ vu}$ ) and the sixth-shortest M(2)–O distance is  $\sim 3.45 \text{ \AA}$  ( $\sim 0.01 \text{ vu}$ ), the latter far too long to be considered as a bond in these structures. Hence the coordination number of M(2) is [5].

First, we consider the bond-valence sums incident at the  $M(1)$  and  $M(3)$  sites as a function of cation coordination-number (Fig. 4). For the  $M(1)$  site, the sum is far below agreement with the valence-sum rule ( $2 \nu u$ , valence units) for a coordination number of [5], and approaches ideality for a coordination number of [8] (Fig. 4a). For the  $M(3)$  site, the sum is far below agreement with the valence-sum rule ( $2 \nu u$ ) for a coordination number of [4], is acceptable for a coordination number of [5], but approaches ideality for a coordination number of [6] (Fig. 4b).

Next, we consider the bond-valence incident at the affected anions (Fig. 5). The bond-valence sums are slightly more in accord with the valence-sum rule for an O(1) coordination of [3], but the deviations for [4]

are also within the normal range for most structures. Similarly for O(5), the values for [3] are slightly to closer to ideal than the values for [4], but it is difficult to persuade oneself that these differences are significant.

In summary, the coordination numbers [8] and [6] result in slightly better bond-valence sums at  $M(1)$  and  $M(3)$  sites than lower coordination numbers, whereas the coordination numbers [7] and [5] at  $M(1)$  and  $M(3)$  result in marginally better bond-valence sums at the O(5) and O(1) sites. We will use the coordination numbers [8], [5], and [6] for the  $M(1)$ ,  $M(2)$ , and  $M(3)$  sites in these minerals and note that the final site-populations were assigned using these values.

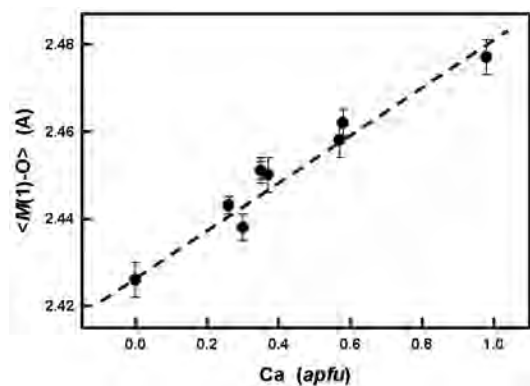


FIG. 1. Variation in  $\langle M(1)-O \rangle$  as a function of Ca content in graftonite-beusite crystals of the present study and those of Steele *et al.* (1991) and Wise *et al.* (1990); the dashed line is drawn as a guide to the eye.

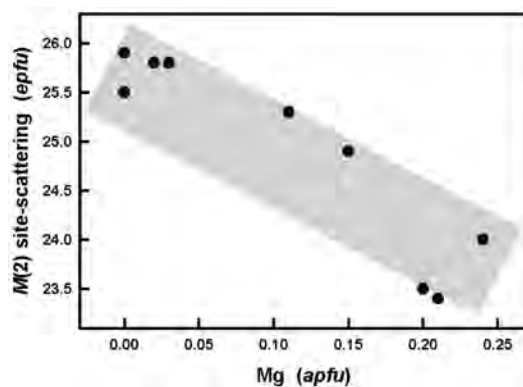


FIG. 2. Variation in refined  $M(2)$ -site scattering as a function of Mg content in graftonite-beusite crystals of the present study and those of Steele *et al.* (1991) and Wise *et al.* (1990); the shaded area shows the scatter involved in possible variation in Mn ( $Z = 25$ ) versus Fe ( $Z = 26$ ).

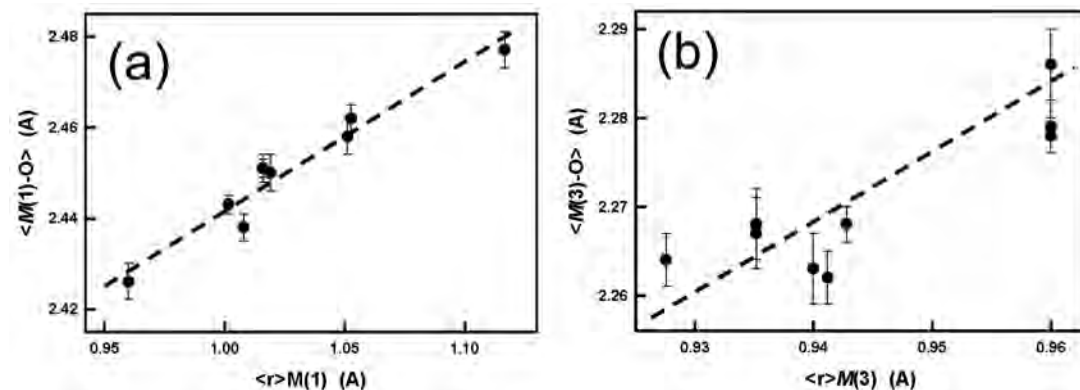


FIG. 3. Variation in (a)  $\langle M(1)-O \rangle$  and (b)  $\langle M(3)-O \rangle$  as a function of constituent M-cation radius; the lines are drawn as a guide to the eye.

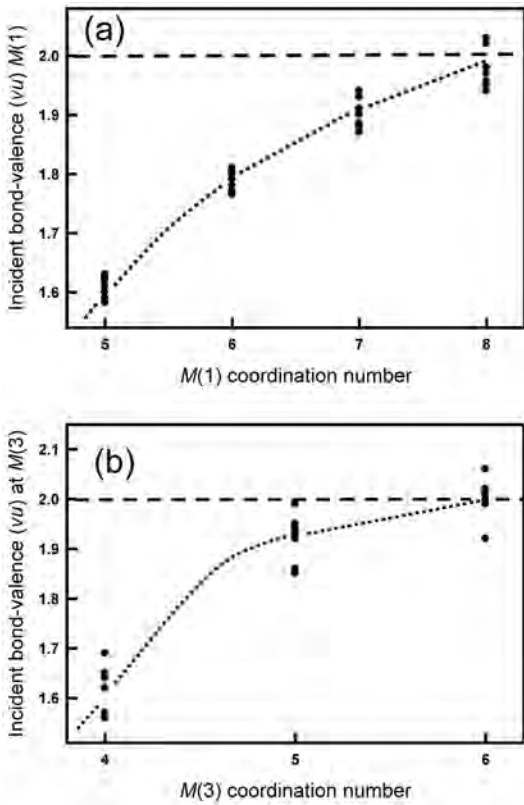


FIG. 4. Variation in incident bond-valence as a function of cation coordination-number at (a) the *M*(1) site, and (b) the *M*(3) site for the crystals of the present study; the dashed line shows accord with the valence-sum rule, and the dotted lines are drawn as guides to the eye.

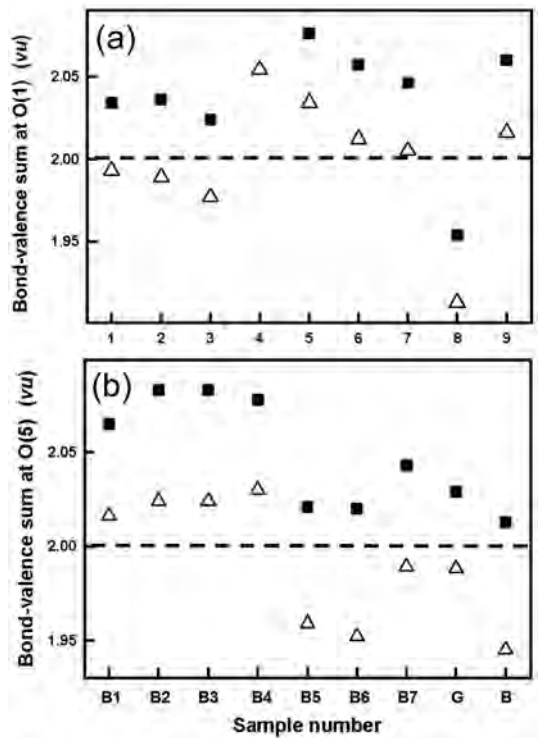


FIG. 5. Variation in incident bond-valence as a function of cation coordination-number at (a) the O(1) anion, and (b) the O(5) anion for graftonite-beusite structures; triangles show [3]-coordination, squares show [4]-coordination, the dashed line shows accord with the valence-sum rule.

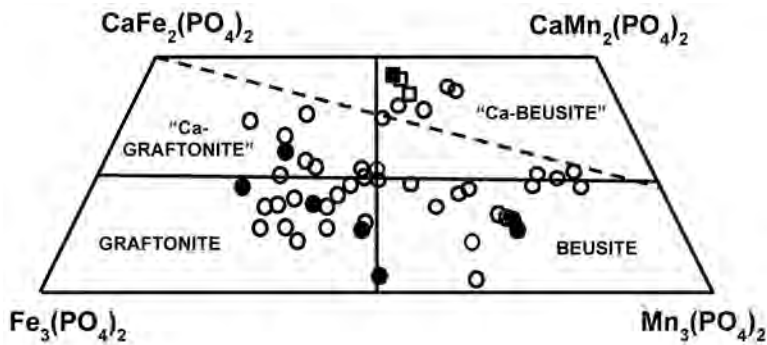


FIG. 6. Composition plot for the  $\text{Fe}_3(\text{PO}_4)$ – $\text{Mn}_3(\text{PO}_4)$ – $\text{CaFe}_2(\text{PO}_4)$ – $\text{CaMn}_2(\text{PO}_4)$  system, showing the ideal compositional fields of graftonite, beusite, “Ca-beusite”, and “Ca-graftonite”; data from Brooks & Shipway (1960), Hurlbut & Aristarain (1968), Franolet *et al.* (1986), Wise & Černý (1990), Staněk (1991), Černý *et al.* (1998), Smeds *et al.* (1998), Piezka (2007) (all white circles), Wise *et al.* (1990) (black square), and this study (black circles).

## DISCUSSION

The complete order of Ca at the  $M(1)$  site is not unexpected, considering the large coordination number of [8] and the large  $\langle M(1)-O \rangle$  distance involving this site. This being the case, it raises the issue of other distinct mineral species with this structure type. Complete order of Ca at  $M(1)$  produces the potential new species "Ca-graftonite" and "Ca-beusite" (note that we are not suggesting that these names ever be validated, but they are a convenient way of discussing these potential minerals). Figure 6 shows the system  $\text{Fe}_3(\text{PO}_4)_2\text{-Mn}_3(\text{PO}_4)_2\text{-CaFe}_2(\text{PO}_4)_2\text{-CaMn}_2(\text{PO}_4)_2$ , together with various compositions within this system reported in the literature. First, there are several compositions within the compositional fields of "Ca-graftonite" and "Ca-beusite", indicating that these are potential new mineral species. Second, the synthesis data of Nord (1982) and Nord & Ericsson (1982) suggest a hypothetical limit of Ca incorporation in the graftonite-beusite structure (indicated by the dashed line in Fig. 6). However, the data of Wise & Černý (1990) suggest that this hypothetical limit of Ca incorporation can be exceeded in minerals. These data are not completely conclusive, and some of the Ca measured by electron microprobe analysis could potentially occur in submicroscopic exsolution lamellae or micro-intergrowths of a more Ca-rich phase. However, the data of Figures 3 and 5 show that the  $\langle M(1)-O \rangle$  distance is linear with Ca content, suggesting that all Ca in the analyses of these crystals occurs at the  $M(1)$  site.

*Site populations in Ca-free beusite*

Steele *et al.* (1991) assigned the following site populations in Ca-free beusite:  $M(1) = M(2) = M(3) = 0.50 \text{ Mn}^{2+} + 0.50 \text{ Fe}^{2+}$ . We may assess these values by calculating the incident bond-valence sums at  $M(1)$ ,  $M(2)$ , and  $M(3)$ ; the resultant values are given in Table 8. There are significant deviations at the  $M(1)$  and  $M(2)$  sites. As these deviations are of opposite sign, they may be reduced by ordering the larger cation at the  $M(1)$  site (as is the case in Ca-bearing beusite)

TABLE 8. BOND-VALENCE SUMS ( $\nu$ ) AT THE  $M$  SITES IN Ca-FREE BEUSITE FOR DIFFERENT SITE-POPULATIONS

	Site population bond-valence	Bond-valence sum at cation
$M(1)$	$\text{Mn}^{2+}_{0.5} + \text{Fe}^{2+}_{0.5}$	1.742
$M(2)$	$\text{Mn}^{2+}_{0.5} + \text{Fe}^{2+}_{0.5}$	2.123
$M(3)$	$\text{Mn}^{2+}_{0.5} + \text{Fe}^{2+}_{0.5}$	1.954
$M(1)$	$\text{Mn}^{2+}$	1.873
$M(2)$	$\text{Fe}^{2+}$	1.962
$M(3)$	$\text{Mn}^{2+}_{0.5} + \text{Fe}^{2+}_{0.5}$	1.954

and the smaller cation at the  $M(2)$  site. Thus assigning only  $\text{Mn}^{2+}$  to  $M(1)$  and only  $\text{Fe}^{2+}$  to  $M(2)$  produces the incident bond-valences shown in Table 8 and reduces significantly the deviation from the valence-sum rule at the  $M(1)$  and  $M(2)$  sites; we suggest that such order is present in Ca-free beusite.

*Cation order in minerals of the graftonite-beusite series*

The linearity in mean bond-length as a function of constituent-cation radius and the adherence of incident bond-valence sums to the valence-sum rule indicate that these minerals show the following site-preferences: Ca:  $M(1)$ ;  $\text{Mn}^{2+}$ :  $M(1) \approx M(3) > M(2)$ ;  $\text{Fe}^{2+}$ :  $M(2) > M(3)$ ; Mg:  $M(2)$ . Note that Ca always occupies  $M(1)$ , and the site preference indicated for  $\text{Mn}^{2+}$  is given for the balance of  $M(1)$  not occupied by Ca. Thus  $M(1)$ : Ca  $\gg$   $\text{Mn}^{2+}$ ;  $M(2)$ :  $\text{Fe}^{2+} > \text{Mn}^{2+}$ ;  $M(3)$ :  $\text{Mn}^{2+} \gg \text{Fe}^{2+}$ .

## ACKNOWLEDGEMENTS

We thank John Hughes and an anonymous reviewer for their comments on this paper. This work was supported by a Canada Research Chair in Crystallography and Mineralogy, and Research Tools and Equipment, Major Facilities Access and Discovery Grants from the Natural Sciences and Engineering Research Council of Canada (NSERC) to FCH, and an NSERC Discovery Grant to KTT.

## REFERENCES

- BEUS, A.A. (1950) Magniophilite and mangankoninckite, two new minerals from pegmatites. *Doklady Akademii Nauk S.S.S.R.* **73**, 1267–1279 (in Russian); *Chemical Abstracts* **45**, 3766.
- BILD, R.W. (1974) New occurrences of phosphates in iron meteorites. *Contributions to Mineralogy and Petrology* **45**, 91–98.
- BROOKS, J.H. & SHIPWAY, C.H. (1960) Mica Creek pegmatites, Mount Isa, North-western Queensland. *Queensland Government Mining Journal* **61(708)**, 511–522.
- BROWN, I.D. (2002) *The Chemical Bond in Inorganic Chemistry: The Bond Valence Model*. Oxford University Press, Oxford, UK.
- BROWN, I.D. & ALTERMATT, D. (1985) Bond-valence parameters obtained from a systematic analysis of the inorganic crystal structure database. *Acta Crystallographica* **B41**, 244–247.
- CALVO, C. (1968) The crystal structure of graftonite. *American Mineralogist* **53**, 742–750.
- ČERNÝ, P., SELWAY, J.B., ERCIT, T.S., BREAKS F.W., ANDERSON, A.J., & ANDERSON, S.D. (1998) Graftonite-beusite in

- granitic pegmatites of the Superior Province: A study in contrasts. *Canadian Mineralogist* **36**, 367–376.
- ERCIT, T.S., TAIT, K.T., COOPER, M.A., ABDU, Y., BALL, N.A., ANDERSON, A.J., ČERNÝ, P., HAWTHORNE, F.C., & GALLISKI, M. (2010) Manitoabaite,  $\text{Na}_{16}\text{Mn}^{2+}_{25}\text{Al}_8(\text{PO}_4)_{30}$ , a new phosphate mineral species from Cross Lake, Manitoba, Canada. *Canadian Mineralogist* **48**, 1455–1463.
- FRANSOLET, A.-M. (1977) Intercroissances et inclusions dans les associations graffonite-sarcopside-triphylite. *Bulletin de la Société Française de Minéralogie et de Cristallographie* **100**, 198–207.
- FRANSOLET, A.-M., KELLER, P., & FONTAN, F. (1986) The phosphate mineral associations of the Tsaobismund pegmatite, Namibia. *Contributions to Mineralogy and Petrology* **92**, 502–517.
- GALLISKI, M.A., OYARZÁBAL, J.C., MÁRQUEZ-ZAVALÍA, M.F., & CHAPMAN, R. (2009) The association qingheite-beusite-lithiophilite in the Santa Ana pegmatite, San Luis, Argentina. *Canadian Mineralogist* **47**, 1213–1223.
- GUASTONI, A., NESTOLA, F., MAZZOLENI, G., & VIGNOLA, P. (2007) Mn-rich graffonite, ferrisicklerite, staněkite and Mn-rich vivianite in a granitic pegmatite at Soè Valley, central Alps, Italy. *Mineralogical Magazine* **71**, 579–585.
- HAWTHORNE, F.C. (1983) Quantitative characterization of site-occupancies in minerals. *American Mineralogist* **68**, 287–306.
- HAWTHORNE, F.C. (1998) Structure and chemistry of phosphate minerals. *Mineralogical Magazine* **62**, 141–164.
- HAWTHORNE, F.C. & SCHINDLER, M. (2008) Understanding the weakly bonded constituents in oxysalt minerals. *Zeitschrift für Kristallographie* **223**, 41–68.
- HAWTHORNE, F.C., UNGARETTI, L., & OBERTI, R. (1995) Site populations in minerals: terminology and presentation of results of crystal-structure refinement. *Canadian Mineralogist* **33**, 907–911.
- HAWTHORNE, F.C., UNGARETTI, L., OBERTI, R., CAUCIA, F., & CALLEGARI, A. (1993) The crystal chemistry of staurolite. I. Crystal structure and site-populations. *Canadian Mineralogist* **31**, 551–582.
- HUMINICKI, D.M.C. & HAWTHORNE, F.C. (2002) The crystal chemistry of the phosphate minerals. *Reviews in Mineralogy and Geochemistry* **48**, 123–253.
- HURLBUT, C.S., JR. & ARISTARAIN, L.F. (1968) Beusite, a new mineral from Argentina, and the graffonite-beusite series. *American Mineralogist* **53**, 1799–1814.
- LAHTI, S.I. (1981) On the granitic pegmatites of the Eräjärvi area in Orivesi, southern Finland. *Bulletin of the Geological Society of Finland* **314**.
- NORD, A.G. (1982) Graffonite-type and graffonite-related  $(\text{Mn}_{1-z}\text{Me}_z)_3(\text{PO}_4)_2$  solid solutions. *Materials Research Bulletin* **17**, 1001–1010.
- NORD, A.G. & ERICSSON, T. (1982) The cation distribution in synthetic  $(\text{Fe},\text{Mn})_3(\text{PO}_4)_2$  graffonite-type solid solutions. *American Mineralogist* **67**, 826–832.
- OLSEN, E.J., KRACHER, A., DAVIS, A.M., STEELE, I.M., HUTCH-  
EON, I.D., & BUNCH, T.E. (1999) The phosphates of IIIAB iron meteorites. *Meteoritics and Planetary Science* **34**, 285–300.
- PENFIELD, S.L. (1900) On graffonite, a new mineral from Grafton, New Hampshire and its intergrowth with triphylite. *American Journal of Science* **159**, 20–32.
- PIECZKA, A. (2007) Beusite and an unusual Mn-rich apatite from the Szklary granitic pegmatite, lower Silesia, southwestern Poland. *Canadian Mineralogist* **45**, 901–914.
- SHANNON, R.D. (1976) Revised effective ionic radii and systematic studies of interatomic distances in halides and chalcogenides. *Acta Crystallographica* **A32**, 751–767.
- SMEDS, S.A., UHER, P., ČERNÝ, P., WISE, M.A., GUSTAFSSON, L., & PENNER, P. (1998) Graffonite – beusite in Sweden: primary phases, products of exsolution, and distribution in zoned populations of granitic pegmatites. *Canadian Mineralogist* **36**, 377–394.
- STALDER, M. & ROZENDAAL, A. (2002) Graffonite in phosphatic iron formations associated with the mid-Proterozoic Gamsberg Zn-Pb deposit, Namaqua Province, South Africa. *Mineralogical Magazine* **66**, 915–927.
- STANĚK, J. (1991) The mineral parageneses of the Dolní Boryhatě pegmatite dykes, western Moravia, Czechoslovakia. *Acta Musei Moraviae, Scientiae Naturales* **76**, 19–49.
- STEELE, I.M., OLSEN, E., PLUTH, J., & DAVIS, A.M. (1991) Occurrence and crystal structure of Ca-free beusite in the El Sempel IIIA iron meteorite. *American Mineralogist* **76**, 1985–1989.
- VIGNOLA, P., DIELLA, V., OPPIZZI, P., TIEPOLO, M., & WEISS, S. (2008) Phosphate assemblages from the Brissago granitic pegmatite, western southern Alps, Switzerland. *Canadian Mineralogist* **46**, 635–650.
- WISE, M.A. & ČERNÝ, P. (1990) Beusite-triphylite intergrowths from the Yellowknife pegmatite field, Northwest Territories. *Canadian Mineralogist* **28**, 133–139.
- WISE, M.A., HAWTHORNE, F.C., & ČERNÝ, P. (1990) Crystal structure of Ca-rich beusite from the Yellowknife pegmatite field, Northwest Territories. *Canadian Mineralogist* **28**, 141–146.

Received March 5, 2013, revised manuscript accepted July 8, 2013.